Journal of proteome research

Article

pubs.acs.org/jpr

High-Performance Chemical Isotope Labeling Liquid Chromatography−Mass Spectrometry for Profiling the Metabolomic Reprogramming Elicited by Ammonium Limitation in Yeast

Xian Luo,[†] Shuang Zhao,[†] Tao Huan,[†] Difei Sun,[†] R. Magnus N. Friis,[‡] Michael C. Schultz,[‡] and Liang Li*[,†]

[†]Department of Chemistry and [‡]Department of Biochemistry, University of Alberta, Edmonton, Alberta, T6G 2R3 Canada

Supporting Information

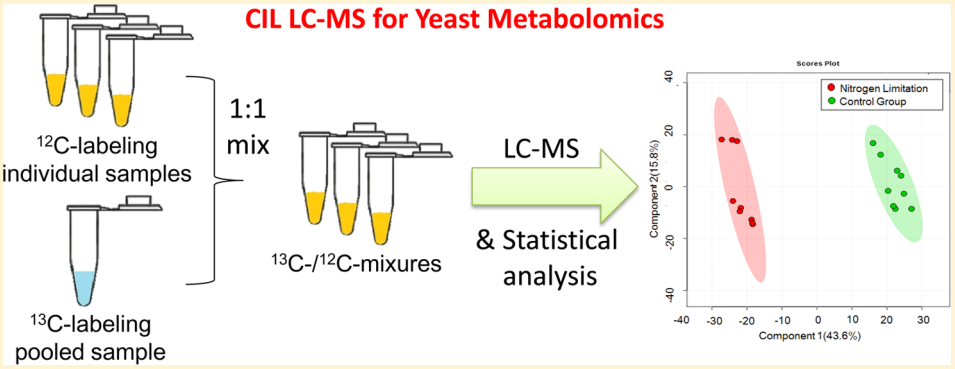

ABSTRACT: Information about how yeast metabolism is rewired in response to internal and external cues can inform the development of metabolic engineering strategies for food, fuel, and chemical production in this organism. We report a new metabolomics workflow for the characterization of such metabolic rewiring. The workflow combines efficient cell lysis without using chemicals that may interfere with downstream sample analysis and differential chemical isotope labeling liquid chromatography mass spectrometry (CIL LC−MS) for in-depth yeast metabolome profiling. Using ^{12}C- and ^{13}C-dansylation (Dns) labeling to analyze the amine/phenol submetabolome, we detected and quantified a total of 5719 peak pairs or metabolites. Among them, 120 metabolites were positively identified using a library of 275 Dns-metabolite standards, and 2980 metabolites were putatively identified based on accurate mass matches to metabolome databases. We also applied ^{12}C- and ^{13}C-dimethylaminophenacyl (DmPA) labeling to profile the carboxylic acid submetabolome and detected over 2286 peak pairs, from which 33 metabolites were positively identified using a library of 188 DmPA-metabolite standards, and 1595 metabolites were putatively identified. Using this workflow for metabolomic profiling of cells challenged by ammonium limitation revealed unexpected links between ammonium assimilation and pantothenate accumulation that might be amenable to engineering for better acetyl-CoA production in yeast. We anticipate that efforts to improve other schemes of metabolic engineering will benefit from application of this workflow to multiple cell types.

KEYWORDS: *yeast, chemical isotope labeling, LC−MS, amine/phenol submetabolome, acid submetabolome, metabolomics*

INTRODUCTION

The yeast species *Saccharomyces cerevisiae* is widely used as a model system for studying biological processes[1] as well as in baking and the production of alcoholic beverages.[2] Improvement of yeast strains used in these traditional applications has shifted from conventional methods for isolation of beneficial variants[3] to directed engineering of desirable metabolic traits.[2,4] The latter metabolic engineering approach is also having a dramatic effect on the development of yeast for more recent industrial applications ranging from biofuel to drug production.[5,6] The workflow in contemporary metabolic engineering projects now often includes broad-coverage metabolic profiling implemented with the goal of determining if and to what extent yeast metabolism is affected by a particular engineering strategy. The information obtained by this approach can guide further engineering steps that improve system performance.[7,8] Therefore, high-coverage quantitative analysis of the yeast metabolome is highly desirable. However, analytical challenges remain in achieving this goal because yeast produces a large range of metabolites of different classes at different concentrations.

There are various analytical platforms used for yeast's metabolome analysis based on NMR[9−11] or mass spectrometry (MS) combined with gas chromatography (GC),[12,13] liquid chromatography (LC),[14−16] and capillary electrophoresis (CE).[17] Among them, LC−MS provides relatively high

Received: January 26, 2016
Published: March 7, 2016

DOI: 10.1021/acs.jproteome.6b00070
J. Proteome Res. 2016, 15, 1602−1612

sensitivity and detectability. However, some challenges still remain for LC−MS. First, ion suppression, matrix effect and instrument drift reduce quantification accuracy and precision. Second, hydrophilic and highly polar metabolites are poorly retained on a reversed-phase chromatography (RPLC) column. Hydrophilic interaction liquid chromatography (HILIC) is required as a complementary technique to separate these metabolites.[18] Both positive and negative ion scans are needed to detect various classes of metabolites. All of these will increase the workload of metabolome analysis. Third, metabolites that have low concentration or low ionization efficiency during electrospray ionization (ESI) will not be detected or detected with low signals, preventing their accurate quantification.

To address these challenges, we have developed a high-performance chemical isotope labeling (CIL) LC−MS platform for quantitative analysis of various submetabolomes with high coverage. For example, differential $^{12}C/^{13}C$-dansylation (Dns) labeling LC−MS is used for profiling the amine/phenol submetabolome,[19] and $^{12}C/^{13}C$-*p*-dimethylaminophenacyl (DmPA) bromide labeling is used for analyzing the carboxylic acid submetabolome.[20] In differential CIL, a ^{12}C-labeling reagent is used to label an individual sample, while a pooled sample produced from mixing equal amounts of aliquots of all individual samples is labeled with the ^{13}C-labeling reagent. The ^{13}C-labeled pool is spiked into an individual ^{12}C-labeled sample, and the mixture is then subjected to LC−MS analysis. The differentially labeled metabolites are detected as peak pairs in mass spectra, and their peak intensity ratio provides the basis for relative quantification. Because the same ^{13}C-labeled pool is used as a reference for all the ^{12}C-labeled individual samples, the peak intensity ratios of a given metabolite reflect the relative concentration difference of the metabolite in the comparative samples. These peak-ratio values can be used for metabolomic comparison using statistical tools. In high-performance CIL LC−MS, the labeling reagents such as Dns and DmPA are rationally designed to alter the metabolite chemical and physical properties to such an extent that simultaneous improvement in separation, detection, and quantification can be achieved. As a result, only RPLC−MS using positive-ion detection is needed. This approach provides a sensitivity improvement of 10- to 1000-fold, allowing the quantification of both high- and low-abundance metabolites.

In this work, we report the development of CIL LC−MS for yeast metabolome analysis with high submetabolome coverage and the application of this method for investigating metabolic reprogramming provoked by removing a nitrogen source from log-phase cells in batch culture. Specifically, cells were switched from high ammonium sulfate medium to medium without ammonium sulfate. We chose to study the effect of ammonium sulfate withdrawal on metabolism for several reasons. First, ammonium sulfate is a high-quality nitrogen source for yeast that on its own can provide all the nitrogen needed for growth.[21,22] Second, physiological homeostasis of yeast and other eukaryotes depends critically on the regulation of nitrogen metabolism. Third, in our experiments, ammonium sulfate withdrawal is expected to affect nitrogen but not sulfate metabolism. That is because the store of sulfate in log-phase cells is likely sufficient for several divisions,[23] and in our experiments, the culture time in 0% ammonium sulfate (6 h) allows for only 2 or 3 divisions.[22] Finally, the amount of ammonium sulfate provided to cells is an important determinant of product yield in yeast that have been metabolically engineered to synthesize biofuels from fatty acids.[24,25] Therefore, information about the metabolic response of cells to ammonium sulfate withdrawal is potentially relevant to the continued development of metabolic engineering strategies in yeast. Because the base medium used in our experiments contains 13 L-amino acids that can support growth,[26] the withdrawal of ammonium sulfate is not expected to trigger a strong physiological response. We chose this modest starvation to determine if CIL LC−MS can provide the necessary sensitivity to confidently identify intercellular metabolites that displayed small changes in abundance in response to a subtle culture manipulation, thereby illustrating the potential general applicability of the developed workflow for yeast metabolomics studies.

EXPERIMENTAL SECTION

Workflow

Figure 1 shows the overall workflow of CIL LC−MS for yeast metabolomics. In general, cells are washed with water and harvested by centrifugation. Washed cell pellets are resuspended in extraction−suspension solvent and lysed by vortexing with glass beads. The lysate is separated from the glass beads and cellular debris, transferred to a new vial, and dried down. The lysates are redissolved in water and subjected to ^{12}C-labeling. The labeled samples are injected into LC−UV to determine the total concentration of labeled metabolites in individual samples for sample amount normalization. On the basis of the total concentration, equal amounts of individual samples are taken and mixed to generate a pooled sample. This pooled sample is labeled using ^{13}C-labeling. Each ^{12}C-labeled individual sample is mixed with an equal amount of the ^{13}C-labeled pool, and the mixture is injected onto LC−MS for metabolite detection and relative quantification. The resultant quantitative metabolomic data are analyzed by using statistical tools to determine the significant metabolites differentiating different groups of cells. These metabolites can be mapped to metabolic pathways for biological studies.

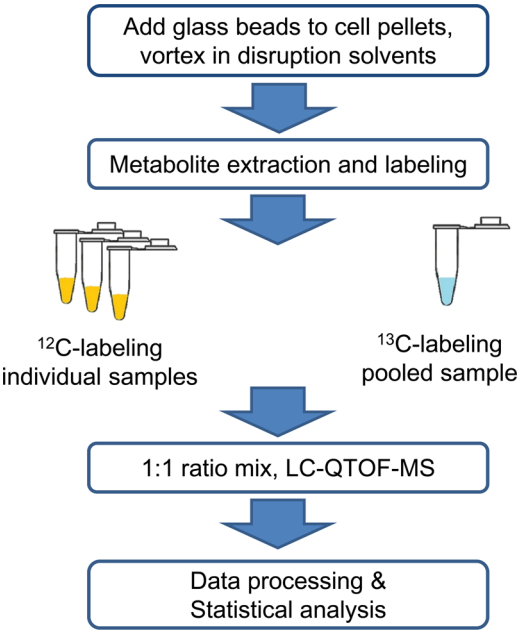

Figure 1. Workflow of the differential chemical isotope labeling (CIL) LC−MS method for yeast metabolomics.

DOI: 10.1021/acs.jproteome.6b00070
J. Proteome Res. 2016, 15, 1602−1612

Chemical and Reagents

All the chemicals and reagents, unless otherwise stated, were purchased from Sigma-Aldrich Canada (Markham, ON, Canada). Glass beads (0.5 mm diameter) were purchased from Biospec Products. ^{13}C-labeling reagents were synthesized in our lab using the procedures published previously[19,20] and are available from MCID.chem.ualberta.ca. LC−MS grade water, formic acid, acetonitrile (ACN), and methanol (MeOH) were purchased from Thermo Fisher Scientific (Edmonton, AB, Canada).

Cell Growth and Cell Lysis

Strain BY4741[27] was selected for this work. BY4741 and its S288c relatives are widely used in metabolic engineering[24,28−32] and, like most laboratory strains, can use ammonium and all the L-amino acids for growth.[21,22] The synthetic culture medium employed here, complete minimal with 2% w/v glucose,[26] contains 0.5% w/v ammonium sulfate as recommended for BY4741;[33] we refer to this medium as CMD+AS. Although CMD+AS contains a high amount of ammonium sulfate, it includes only a subset of amino acids. This amino acid formulation is preferred for BY4741 because its proliferation is inhibited in synthetic media containing all amino acids.[34] Cells were cultured to mid-log-phase CMD+AS at 30 °C and 225 rpm in a shaking incubator for 24 h. The medium was replaced with fresh CMD+AS (control group) or CM without ammonium sulfate +2% glucose (CMD−AS; nitrogen starvation group), and cultures were returned to the 30 °C shaking incubator. The cells were harvested by centrifugation (4640*g* for 10 min at 4 °C) 6 h after resuspension in fresh medium. The pellets were resuspended in 1 mL of cold water (LC−MS grade) and spun in an Eppendorf 5415C microcentrifuge at 16000*g* for 1 min at 4 °C. After removing the water, we repeated this washing process two more times to remove excess growth medium. After the removal of the water, the final cell pellets were snap-frozen in liquid nitrogen and then stored at −80 °C until further use.

For cell lysis, 0.5 cc (mL) of glass beads and 100 μL of extraction/suspension solvent (MeOH or ACN in water; see the Results section) were added to a 1.5 mL microcentrifuge tube that contained the frozen cell pellets. Cell lysis was achieved via five 1 min periods of bead-beating at 3200 rpm using a VORTEX-GENIE 2 Mixer (Fisher Scientific) alternated with five 1 min incubations in an ice−water bath. After cell lysis, another 800 μL of extraction solvent was added for metabolite extraction. To determine the percent cell breakage, we counted cells with hemocytometer under a LEICA DM 1L inverted contrasting microscope (Wetzlar, Germany). Unbroken cells and cell debris were removed by centrifugation at 16000*g* at 4 °C for 10 min, and the supernatant was transferred to a new vial and dried down in a Savant SC110A Speed Vac at room temperature. Drying metabolite extracts at room temperature was used by others.[35] After metabolite extraction, the metabolite levels were not expected to be affected by the sample drying process, as most of the enzymes should be removed. The dried metabolites were redissolved in LC−MS grade water and stored at −80 °C.

Dansylation Labeling

A total of 25 μL of the metabolite extract was mixed with 12.5 μL of sodium carbonate/sodium bicarbonate buffer and 12.5 μL of ACN. The solution was spun down and mixed with 25 μL of freshly prepared ^{12}C-dansyl chloride solution (18 mg/mL in ACN) (for light labeling) or ^{13}C-dansyl chloride solution (18 mg/mL in ACN) (for heavy labeling). The reaction was allowed to proceed for 1 h at 40 °C. After 1 h, 5 μL of 250 mM NaOH was added to the reaction mixture to quench the excess dansyl chloride. The solution was then incubated at 40 °C for another 10 min. Finally, 25 μL of formic acid in 1:1 ACN/H_2O was added to consume excess NaOH and to acidify the solution.

DmPA Bromide Labeling

Prior to isotopic labeling, a liquid−liquid extraction step was carried out to remove amine-containing compounds to increase the specificity of the reaction for carboxylic acids.[36] Cellular metabolites were extracted with 150 μL of ethyl acetate. The organic layer was dried and dissolved in 30 μL of 20 mg/mL triethylamine and then mixed with 30 μL of freshly prepared ^{12}C-DmPA bromide solution (20 mg/mL in ACN) (light labeling) or ^{13}C-DmPA bromide solution (20 mg/mL in ACN) (heavy labeling). The reaction was incubated at 85 °C for 60 min.

LC−UV Quantification

A LC−UV quantification step was carried out prior to mass analysis to control the amount of sample used for metabolome comparison (i.e., sample normalization).[37] A total of 2 μL of the labeled solution was injected onto a Phenomenex Kinetex C18 column (2.1 mm × 5 cm, 1.7 μm particle size, 100 Å pore size) linked to a Waters ACQUITY UPLC system (Waters, Milford, MA) for step-gradient LC−UV. The UV detector was operated at 338 nm. Solvent A was 0.1% (v/v) formic acid in 5% (v/v) ACN, and solvent B was 0.1% (v/v) formic acid in acetonitrile. The gradient started with 100% A for 1 min and was increased to 95% B within 0.1 min and held at 95% B for 1.5 min. The gradient was restored to 100% A in 0.5 min and held at this condition for 3 min to re-equilibrate the column. The flow rate used was 0.45 mL/min.

LC−MS

The ^{13}C-labeled pool was mixed with an equal amount of the ^{12}C-labeled individual sample and the mixture was analyzed using a Bruker Impact HD quadrupole time-of-flight (Q-TOF) mass spectrometer (Bruker, Billerica, MA) linked to an Agilent 1100 series binary HPLC system (Agilent, Palo Alto, CA). The samples were injected onto an Agilent reversed-phase Eclipse Plus C18 column (2.1 mm × 10 cm, 1.8 μm particle size, 95 Å pore size) for separation. Solvent A was 0.1% (v/v) formic acid in 5% (v/v) acetonitrile, and solvent B was 0.1% (v/v) formic acid in acetonitrile. The chromatographic conditions for dansyl labeling were: t = 0 min, 20% B; t = 3.5 min, 35% B; t = 18 min, 65% B; t = 21 min, 95% B; t = 26 min, 95% B. The gradient for DmPA labeling was t = 0 min, 20% B; t = 9 min, 50% B; t = 22 min, 65% B; t = 26 min, 80% B; t = 29 min, 98% B; t = 40 min, 98% B. The flow rate was 180 μL/min. All MS spectra were obtained in the positive ion mode. The MS conditions used for Q-TOF were as follows: nebulizer, 1.0 bar; dry temperature, 230 °C; dry gas, 8 L/min; capillary voltage, 4500 V; end plate offset, 500 V; spectra rate, 1.0 Hz.

Data Processing and Analysis

A software tool, IsoMS,[38] was used to process the raw data generated from multiple LC−MS runs by peak picking, peak pairing, peak-pair filtering, and peak-pair intensity ratio calculation. After the alignment of multiple data files by retention time and accurate mass, missing values in the aligned files were filled by the Zerofill program.[39] The data file was uploaded to the MetaboAnalyst Web site (www.metaboanalyst.

DOI: 10.1021/acs.jproteome.6b00070
J. Proteome Res. 2016, 15, 1602−1612

ca), and multivariate statistical analysis was performed. Principal component analysis (PCA), partial least-squares discriminant analysis (PLS-DA), and heatmapping were used to analyze the data. Volcano plots and box plots were generated using Origin 9.0. Metabolite identification was performed based on accurate mass and retention time match to a dansyl or DmPA standard library.[40] Putative identification was done based on accurate mass match to the metabolites in the yeast metabolome database (YMDB) (www.ymdb.ca), the human metabolome database (HMDB) (www.hmdb.ca), and the predicted human metabolite library in MyCompoundID (MCID) (www.mycompoundid.org).[41]

RESULTS AND DISCUSSION

Cell Lysis for Metabolomic Analysis

Efficient and complete cell lysis is critical to generate the metabolome profile that reflects the whole cell population. If only a fraction of cells are lysed, only a partial population is investigated, leaving one to wonder if the unlysed cells might have different metabolomic compositions than the lysed ones. Another critical consideration is related to the use of chemicals for cell lysis. It is important not to use any chemicals that may cause interference in downstream sample processing, such as chemical labeling and LC−MS analysis. In our work, we chose to employ a glass-bead-assisted cell lysis method to obtain intracellular metabolites from yeast. Using this method, LC−MS analysis can be conducted using metabolites extracted from the cells harvested from <1 mL of culture. We have optimized this bead method, including the cell extraction−suspension solution and lysis condition, to achieve high-yield cell lysis.

Figure 2A,B shows the microscopy images of cells. The control group was vortexed in 50% MeOH without glass beads for five rounds, and the disruption group was vortexed with glass beads in 50% MeOH. The intact cells can refract light and appear as bright dots, while the cell debris appears as dark dots. Almost all of the cells were cracked after five rounds of vortexing with glass beads in MeOH. Because one cell may break and generate several pieces of debris, directly calculating the ratio of intact cells (light dots) to black dots after lysis would generate an artificially high estimate of cell lysis efficiency. In our work, the cell breakage percentage was determined by the number of intact cells before and after lysis.

Because methanol and acetonitrile are widely used as solvents in cell lysis and metabolites extraction, we compared four solvents (50% MeOH, 80% MeOH, 50% ACN, and 80% ACN) to see which gives the best cell lysis efficiency using the bead method. The results are plotted in Figure 2C. Among them, the 50% MeOH group showed the highest cell lysis efficiency with 96.1% of cells lysed. The lowest efficiency group was 80% ACN with only 15.9% lysis efficiency. The efficiency of using 80% MeOH (76.6%) was higher than that of using 50% ACN (58.6%). The solvent dependence of lysis efficiency may be attributed to the different levels of cell suspension and clumping in different solvents. In the bead-beating method, agitation by vortexing causes beads to collide with cells and crack their walls, and thus, a solvent offering the best dispersal of cells in suspension likely provides the most efficient cell lysis. In all of the subsequent experiments, the glass-bead method using 50% MeOH for cell suspension was used for cell lysis, which is fully compatible with downstream labeling and LC−MS analysis.

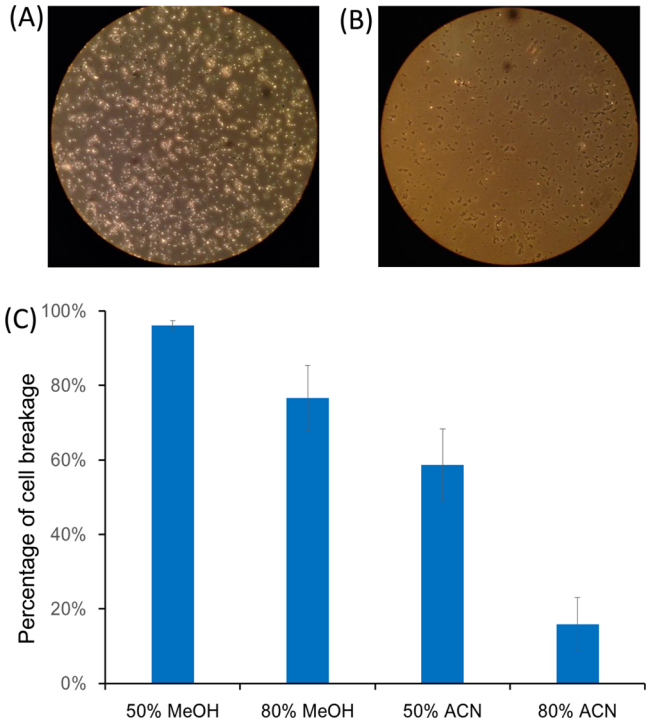

Figure 2. Microscopy images of cell lysis: (A) control group without glass beads; the yeast cells remained intact after vortexing. (B) Disruption group with glass beads in 50% MeOH after vortexing; cell debris were shown as dark dots. (C) Comparison of cell lysis efficiency of four different solvents. Cell counting with hemocytometer was used to determine the percentage of cell breakage (n = 3).

Analysis of Amine- and Phenol-Containing Metabolites

The amine-containing metabolites play an important role in metabolic pathways. For example, the 275 amines and phenols in the current Dns-metabolite standard library cover 43 different metabolic pathways. Most of the metabolites in amino-acid metabolic pathways and nucleotide metabolic pathways are amine-containing metabolites. Phenol-containing metabolites are common in tyrosine, phenylalanine, and tryptophan metabolic pathways. Thus, dansylation LC−MS offers a way to figure out how the nitrogen starvation affects these metabolic pathways.

On average, 3763 ± 271 peak pairs were detected in triplicate experiments on biological triplicate samples of the ammonium limitation group and control-group lysates. In total, there were 5719 peak pairs or metabolites detected from all of the samples combined. The IsoMS program filtered out all the adducts, dimers, multimers, etc., in mass spectra to retain only the $[M + H]^+$ peak pairs, and thus, in most cases, each pair represents a unique metabolite; in cases of a metabolite containing more than one amine or phenol group, multiple products may be generated. We performed metabolite identification based on mass and retention time match to a dansyl library containing 275 metabolite standards.[40] A total of 120 metabolites were positively identified, and they are listed in Table 1. Detailed information on the matches is shown in Supplemental Table S1. We also searched the accurate masses of the detected metabolites against the HMDB database and found 926 matches (see Supplemental Table S2). In addition, using the MCID library with one reaction, we further matched 1857 metabolites (see Supplemental Table S3). Thus, among the 5719 peak pairs found, we could match 3040 metabolites (i.e.,

DOI: 10.1021/acs.jproteome.6b00070
J. Proteome Res. 2016, 15, 1602−1612

Table 1. List of Amine- or Phenol-Containing Metabolites Identified

no.	HMDB ID	name	no.	HMDB ID	name
1	HMDB29306	4-ethylphenol	61	HMDB00721	glycylproline
2	HMDB29118	tyrosyl-valine	62	HMDB00719	homoserine
3	HMDB29109	tyrosyl-leucine	63	HMDB00719	homoserine−H_2O
4	HMDB29105	tyrosyl-glycine	64	HMDB00706	aspartyl-phenylalanine
5	HMDB29098	tyrosyl-alanine	65	HMDB00696	methionine
6	HMDB29095	tryptophyl-tyrosine	66	HMDB00687	leucine
7	HMDB29065	threoninyl-leucine	67	HMDB00669	ortho-hydroxyphenylacetic acid
8	HMDB29007	phenylalanyl-tyrosine	68	HMDB00650	α-aminobutyric acid
9	HMDB28988	phenylalanyl-alanine	69	HMDB00641	glutamine
10	HMDB28941	leucyl-tyrosine	70	HMDB00557	alloisoleucine
11	HMDB28937	leucyl-proline	71	HMDB00517	arginine
12	HMDB28878	histidinyl-alanine	72	HMDB00500	4-hydroxybenzoic acid
13	HMDB28854	glycyl-valine	73	HMDB00469	5-hydroxymethyluracil
14	HMDB28848	glycyl-phenylalanine	74	HMDB00455	allocystathionine
15	HMDB28844	glycyl-isoleucine	75	HMDB00455	allocystathionine isomer
16	HMDB28694	alanyl-phenylalanine	76	HMDB00452	α-aminobutyric acid
17	HMDB28691	alanyl-leucine	77	HMDB00450	5-hydroxylysine
18	HMDB28689	alanyl-histidine	78	HMDB00446	*N*-α-acetyllysine
19	HMDB13243	leucyl-phenylalanine	79	HMDB00440	3-hydroxyphenylacetic acid
20	HMDB11737	γ glutamylglutamic acid	80	HMDB00301	urocanic acid
21	HMDB11177	phenylalanyl-proline	81	HMDB00300	uracil
22	HMDB06050	*o*-tyrosine	82	HMDB00296	uridine
23	HMDB04987	α-aspartyl-lysine	83	HMDB00296	uridine−H_2O
24	HMDB03911	3-aminoisobutanoic acid	84	HMDB00292	xanthine
25	HMDB03464	4-guanidinobutanoic acid−H_2O	85	HMDB00279	saccharopine
26	HMDB03423	glutamine	86	HMDB00279	saccharopine−H_2O
27	HMDB03337	oxidized glutathione	87	HMDB00228	phenol
28	HMDB03320	indole-3-carboxylic acid	88	HMDB00214	ornithine
29	HMDB03012	aniline	89	HMDB00210	pantothenic acid
30	HMDB02658	6-hydroxynicotinic acid	90	HMDB00206	N_6-acetyl-lysine
31	HMDB02393	*N*-methyl-aspartic acid	91	HMDB00191	aspartic acid
32	HMDB02390	3-cresotinic acid	92	HMDB00182	lysine
33	HMDB02362	2,4-diaminobutyric acid	93	HMDB00177	histidine
34	HMDB02322	cadaverine	94	HMDB60003	isovanillic acid
35	HMDB02141	*N*-methyl-α-aminoisobutyric acid	95	HMDB00172	isoleucine
36	HMDB02064	N-acetylputrescine	96	HMDB00168	asparagine
37	HMDB02005	methionine sulfoxide	97	HMDB00168	asparagine−H_2O
38	HMDB02005	methionine sulfoxide isomer	98	HMDB00167	threonine
39	HMDB01964	caffeic acid	99	HMDB00162	proline
40	HMDB01906	2-aminoisobutyric acid	100	HMDB00161	alanine
41	HMDB01891	*m*-aminobenzoic acid	101	HMDB00159	phenylalanine
42	HMDB01842	guanidine	102	HMDB00158	tyrosine
43	HMDB01545	pyridoxal	103	HMDB00157	hypoxanthine - multitags
44	HMDB01431	pyridoxamine	104	HMDB00149	ethanolamine
45	HMDB01414	1,4-diaminobutane	105	HMDB00148	glutamic acid−H_2O
46	HMDB01392	*p*-aminobenzoic acid	106	HMDB00148	glutamic acid
47	HMDB01257	spermidine	107	HMDB00133	guanosine
48	HMDB01232	4-nitrophenol	108	HMDB00123	glycine
49	HMDB01173	5′-methylthioadenosine	109	HMDB00112	γ-aminobutyric acid
50	HMDB01149	5-aminolevulinic acid	110	HMDB00112	γ-aminobutyric acid - H_2O
51	HMDB01065	2-hydroxyphenethlamine - Isomer	111	HMDB00101	deoxyadenosine
52	HMDB01049	γ-glutamylcysteine	112	HMDB00099	cystathionine isomer
53	HMDB00957	pyrocatechol	113	HMDB00099	cystathionine
54	HMDB00929	tryptophan	114	HMDB00070	pipecolic acid
55	HMDB00883	valine	115	HMDB00056	β-alanine
56	HMDB00819	normetanephrine	116	HMDB00050	adenosine
57	HMDB00763	5-hydroxyindoleacetic acid	117	HMDB00045	adenosine monophosphate
58	HMDB00759	glycyl-leucine	118	HMDB00020	*p*-hydroxyphenylacetic acid
59	HMDB00755	cydroxyphenyllactic acid	119	316000000*	phenyl-leucine
60	HMDB00750	3-hydroxymandelic acid	120	HMDB00750	3-hydroxymandelic acid−COOH

DOI: 10.1021/acs.jproteome.6b00070
J. Proteome Res. 2016, 15, 1602−1612

Table 1. continued

*This metabolite does not have an HMDB number but is present in the dansyl standards library. The number shown is a designated number in the dansyl standards library.

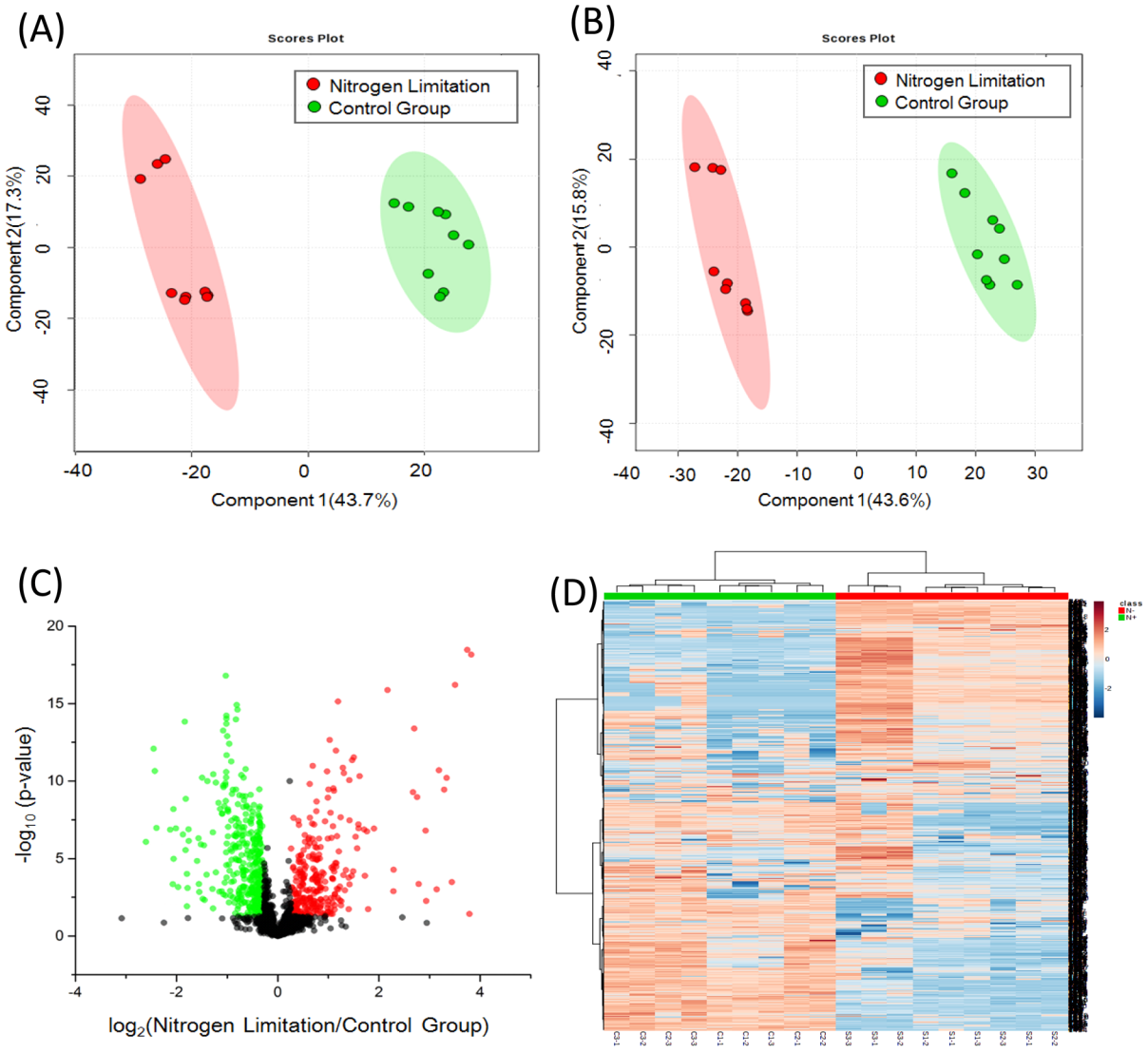

Figure 3. Score plots of (A) PCA and (B) PLS-DA of dansylation-labeled lysates from *S. cerevisiae* cultured with or without ammonium limitation. The data was from experimental triplicates on biological triplicate samples. (C) Volcano plot of the changes of amine- and phenol-containing metabolites. The up-regulated or down-regulated metabolites by at least 1.2-fold, with p values of smaller than 0.05, are marked in red and green, respectively. (D) Clustered heatmap showing the comparison of the relative intensity of each peak pair in the nitrogen limitation group and the control group.

53%). It should be noted that we also searched the yeast metabolome database (YMDB), which is much smaller than HMDB. We matched 672 metabolites in YMDB using mass search. Among them, only eight metabolites were uniquely found in YMDB, while 664 metabolites overlapped with the human metabolites (see Supplemental Table S4−1). These eight unique metabolites could be matched to the MCID library. Thus, the use of YMDB did not yield any additional matches. On the basis of the large number of peak pairs detected and metabolite matches found, it is clear that the yeast metabolome is very complex. Unfortunately, there are a limited number of metabolite standards currently available to confirm the identities of the putatively matched metabolites. The future work of confirming these identities may lead to the discovery of new intermediates in known pathways as well as revealing totally unknown metabolic pathways.

Using the data generated by dansylation LC−MS, PCA and PLS-DA were first applied to evaluate whether ammonium starvation affects the metabolomic profiles of *S. cerevisiae*; the relevant score plots are shown in Figure 3A,B. The two groups with and without the ammonium starvation can be well separated. In the PCA plot, 43.7% and 17.3% variances were captured by the first principal component (1st PC) and the second PC, respectively. Most variances were captured by the first two components reflected a good quality of the model. This was further validated in the cross-validation test for the PLS-DA model as R^2 = 0.999 and Q^2 = 0.981.

DOI: 10.1021/acs.jproteome.6b00070
J. Proteome Res. 2016, 15, 1602−1612

Table 2. List of Carboxylic-Acid-Containing Metabolites Identified

no.	HMDB ID	name	no.	HMDB ID	name
1	HMDB00634	citraconic acid	18	HMDB00892	valeric acid
2	HMDB00202	methylmalonic acid	19	HMDB00718	isovaleric acid
3	HMDB01987	2-hydroxy-2-methylbutyric acid	20	HMDB00134	fumaric acid
4	HMDB00440	3-hydroxyphenylacetic acid	21	HMDB00695	methyloxovaleric acid
5	HMDB02466	3-hydroxybenzoic acid	22	HMDB00408	2-methyl-3-ketovaleric acid
6	HMDB00576	ethyl malonate	23	HMDB00689	isocaproic acid
7	HMDB01975	2-ethyl-2-hydroxybutyric acid	24	HMDB02097	4-ethylbenzoic acid
8	HMDB00858	monomethyl glutaric acid	25	HMDB00666	heptanoic acid
9	HMDB02428	terephthalic acid	26	HMDB00784	azelaic acid
10	HMDB00669	hydroxyphenylacetic acid	27	HMDB00392	2-octenoic acid
11	HMDB00254	succinic acid	28	HMDB01877	valproic acid
12	HMDB00955	3-hydroxy-4-methoxycinnamic aicd	29	HMDB00847	nonanoic acid
13	HMDB00779	phenyllactic acid	30	HMDB00623	dodecanedioic acid
14	HMDB00209	phenylacetic acid	31	HMDB00511	capric acid
15	HMDB00208	oxoglutaric acid	32	HMDB00529	5-dodecenoic acid
16	HMDB01870	benzoic acid	33	HMDB00638	dodecanoic acid
17	HMDB02176	ethylmethylacetic acid			

We also analyzed the data using a Volcano plot that combines the fold-change and the p value from a t test to determine the significant metabolites that separate the two groups. The Volcano plot is shown in Figure 3C using thresholds of ≥1.2-fold change and p value of ≤0.05. There were 603 peak pairs up-regulated and 706 peak pairs down-regulated in response to nitrogen limitation (see Supplemental Table S5−1 for a list of positively identified metabolites and Supplemental Table S5−2 for a list of putatively identified metabolites). To compare the intensity change of each metabolite, we generated a heatmap (see Figure 3D) with deeper red representing higher intensity and deeper blue representing lower intensity. The color distribution is similar within each group but very different between the groups, indicating that there are characteristic and reproducible differences between the metabolic programs of yeast cultured in the presence or absence of ammonium sulfate. All of these statistical analyses show that the amine/phenol submetabolome of *S. cerevisiae* changes significantly in response to nitrogen starvation, and the CIL LC−MS method can reveal the change of a large number of metabolites.

Analysis of Carboxylic-Acid-Containing Metabolites

Carboxylic acid containing metabolites are another important submetabolome in metabolic pathways. Among the cellular metabolites of central carbon metabolism, there are multiple carboxylic acids including di-, tri-, and keto-carboxylic compounds.[42] Some of these are intermediates in the tricarboxylic acid (TCA) cycle, which is a core pathway for the metabolism of sugars, amino acids, and lipids.[43] To analyze this submetabolome, we used DmPA bromide labeling method to increase the detection sensitivity of these metabolites.

An average of 1961 ± 71 peak pairs or metabolites were detected from triplicate experiments on biological triplicate samples of the nitrogen limitation group and the control group. In total, 2286 peak pairs were detected. Identification of carboxylic acid-containing metabolites was performed based on mass and retention time match to a DmPA standard library containing 188 acid standards. A total of 33 metabolites were positively identified, and they are shown in Table 2. Supplemental Table S6 lists more information on the matches. By searching accurate masses of the remaining peak pairs, we found 248 matches to the metabolites in HMDB and 1347 matches to the MCID library (see Supplemental Table S7 and S8) for a total of 1595 matches representing 70% of the 2286 peak pairs detected. Using the yeast database, we matched 133 metabolites, and among them, only 11 metabolites were not found in HMDB (see Supplemental Table S4−2). However, these 11 unique metabolites could be found in the MCID library. As in the case of analyzing the amine/phenol submetabolome, searching YMDB did not generate any additional match. The large number of metabolites detected in this acid submetabolome profiling work suggests again that the composition of the yeast metabolome is complex. Many of the acid-containing metabolites remain to be positively identified.

This acid submetabolome data set was examined using PCA and PLS-DA. The PCA plot (see Figure 4A) indicates that the separation of the starvation and control groups based on the first and second PCs is not as large as that in the amine/phenol submetabolome. However, the two groups are well-separated on the basis of the second and third PCs (Figure 4B). There were 31.8%, 11.6%, and 10.9% of variances captured by the first, second, and third PC, respectively. We also applied PLS-DA to evaluate the starvation and control groups. As shown in Figure 4C, there is a clear distinction between the ammonium limitation group and the control group (R^2 = 0.999 and Q^2 = 0.873). However, a lower percentage (11.6%) of variances was captured by the first PC compared to the amine/phenol submetabolome, which suggests that the extent of the acid submetabolome change is less than that of the amine/phenol submetabolome. This conclusion is supported by the Volcano plot shown in Figure 4D. Using thresholds of ≥1.2-fold change and p value of ≤0.05, there are only 83 metabolites up-regulated and 189 metabolites down-regulated (see Supplemental Table S5−1 for a list of positively identified metabolites and Supplemental Table S5−3 for a list of putatively identified metabolites). These numbers are much less than the number of changed amine/phenol metabolites. Nevertheless, these changes still reflect a large difference in acid submetabolome between the two groups. The sensitive CIL LC−MS method with high-coverage submetabolomic profiling allows the detection of these changes.

DOI: 10.1021/acs.jproteome.6b00070
J. Proteome Res. 2016, 15, 1602−1612

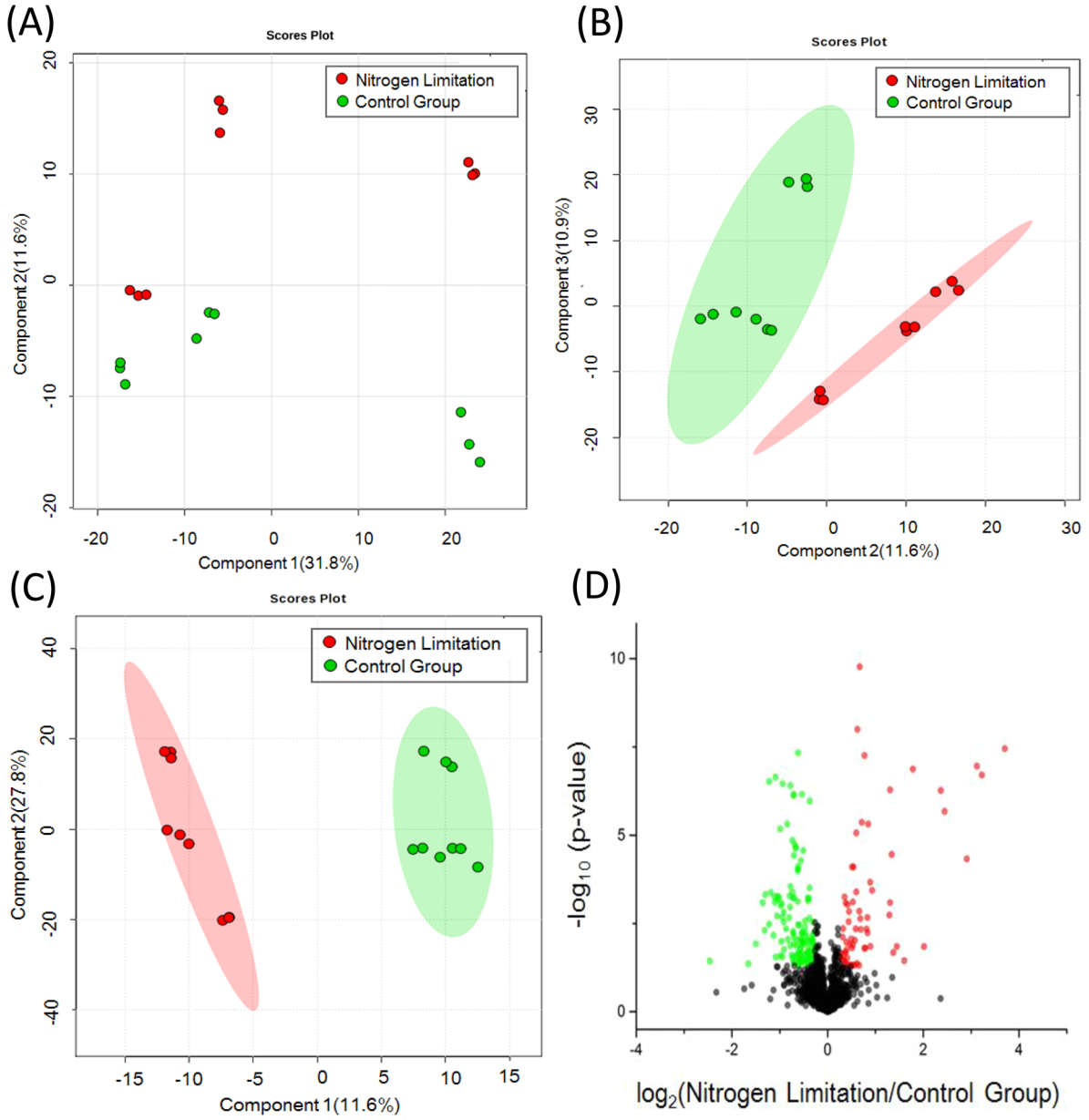

Figure 4. (A) PC1 versus PC2 PCA score plot, (B) PC2 versus PC3 PCA score plot, and (C) PLS-DA score plot of DmPA labeled lysates from *S. cerevisiae* cultured with or without ammonium limitation. The data was from experimental triplicates on biological triplicate samples. (D) Volcano plot of the changes of carboxylic acid-containing metabolites. The up-regulated or down-regulated metabolites by at least 1.2-fold, with p values of smaller than 0.05, are marked in red and green, respectively.

Metabolic Pathway Analysis

The large coverage of amine/phenol and acid submetabolomes enables us to examine some of the metabolic pathways significantly altered by ammonium starvation. Budding yeast is well equipped to fine-tune its metabolism to fluctuations in nitrogen source availability. The way that metabolism is reprogrammed by nitrogen source fluctuation depends on whether its quality or amount changes.[21] In our experiment, the nitrogen source manipulation is not dramatic: the removal of ammonium, a preferred nitrogen source, but not amino acids that can be used in its stead. The CIL LC−MS data support the prediction that metabolic reprogramming under this condition is modest. For example, although complete nitrogen withdrawal is associated with α-ketoglutarate induction signaling ammonia deprivation,[44] withdrawal of just ammonium sulfate has little, if any, effect on ammonium (1.17-fold increase at 6 h in CMD-AS, $p = 4.32 \times 10^{-2}$) and causes depletion of α-ketoglutarate (oxoglutarate, see Figure 5).

The most informative changes in metabolite abundance associated with ammonium sulfate limitation are shown in Figure 5 (fold changes are the CMD−AS/CMD+AS ratios). These include depletion of arginine and its immediate precursor L-arginino-succinate with a concurrent increase in ornithine levels. Changes in polyamine metabolism fed by arginine catabolism, are also associated with ammonium starvation (see Figure 5). There is the buildup of two products derived from the ornithine breakdown product putrescine; *N*-acetyl-putrescine and spermidine. It seems likely that increased levels of these metabolites were primarily due to increased arginine degradation rather than an increase in the activity of the enzymes that act on putrescine. The enzyme responsible for

DOI: 10.1021/acs.jproteome.6b00070
J. Proteome Res. 2016, 15, 1602−1612

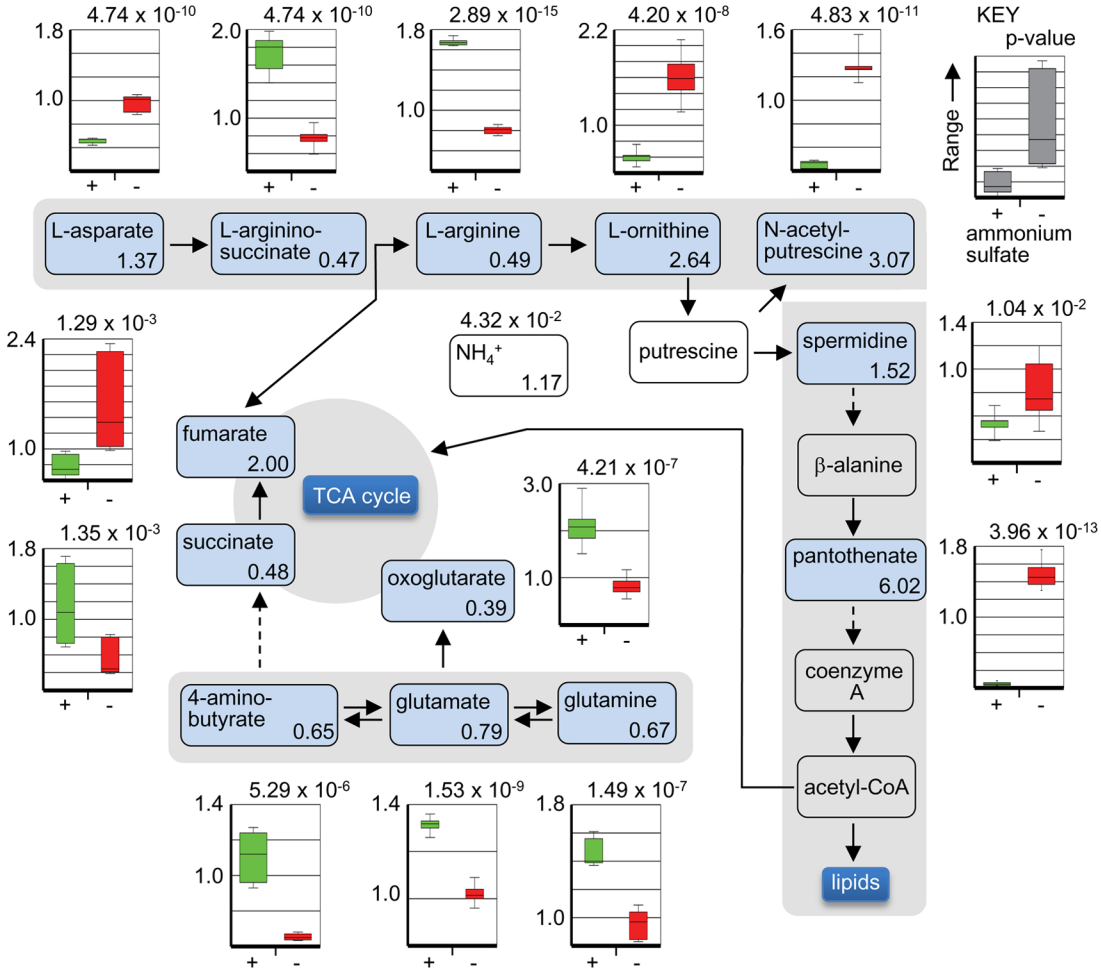

Figure 5. Metabolite changes in selected metabolic pathways. The graphs are for selected metabolites (blue shading) that differ significantly in abundance ($p \leq 0.05$) between cells cultured with or without ammonium limitation. Fold differences in abundance are given in the name boxes for the metabolites.

acetylation of putrescine also acetylates spermidine and spermine, and overexpression of this enzyme causes depletion of all three of these polyamines.[45] Similarly, the overexpression of an enzyme in the pathway of polyamine catabolism in mammalian cells causes accumulation of a polyamine catabolic intermediate and drawing down of spermine and spermidine.[46] Accumulation of *N*-acetyl-putrescine in ammonium-starved yeast cells is not associated with the depletion of spermidine or spermine; spermidine in fact accumulates (Figure 5). This finding suggests that in response to ammonium limitation, increased arginine catabolism: 1) accounts for its decreased steady-state abundance, and 2) feeds increased biosynthesis of spermidine which can be utilized for the generation of pantothenate, the most highly induced metabolite.

The strongest effect of ammonium starvation on metabolite abundance is the 6-fold induction of pantothenate (Figure 5). This induction is potentially linked to the metabolism of aspartate and arginine because pantothenate biosynthesis can involve the conversion of these amino acids to ornithine, followed by spermine production in a subpathway that generates pantothenate (Figure 5). Pantothenate is in the biosynthetic pathway for acetyl-CoA, a central intermediate in overall metabolism.[47,48] The fact that pantothenate accumulates in ammonium-starved cells raises the possibility that altered nitrogen metabolism affects the flux through pathways that require acetyl-CoA. Because a large number of compounds targeted for production in engineered yeast require acetyl-CoA for their synthesis, strategies for achieving high acetyl-CoA yield from glucose have been and continue to be developed.[49−52] Our evidence that ammonium limitation has a strong effect on pantothenate metabolism raises the possibility that systems engineering for the optimal production of acetyl-CoA could benefit from interventions that target this axis of metabolism.

All of the nitrogen in the macromolecular constituents of yeast cells is derived from glutamate and glutamine, which themselves are formed by reactions in which ammonium is the nitrogen donor.[22,53] CMD contains glutamate but not glutamine. Therefore, in CMD+AS and CMD−AS scenarios, cells must use ammonium and glutamate to produce the glutamine required for synthesis of asparagine, tryptophan, purines and pyrimidines.[22] It follows that ammonium starvation likely affects the abundance of molecules in this module of metabolism. Indeed, there are modest changes in the abundance of glutamate and three molecules it can be used to make: glutamine, 2-oxoglutarate (α-ketoglutarate), and 4-aminobutyrate (GABA) (see Figure 5). Because 2-oxoglutarate is a key intermediate in the TCA cycle, it is not surprising that other TCA intermediates (succinate and fumarate) also change in abundance in response to ammonium starvation (Figure 5). Indeed, the buildup of fumarate may be causally related to

DOI: 10.1021/acs.jproteome.6b00070
J. Proteome Res. 2016, 15, 1602−1612

depletion of two of its precursors, succinate in the TCA cycle and L-arginino-succinate in the pathway of arginine synthesis (Figure 5). The steady-state metabolite abundance data we have obtained will provide a starting point for metabolic flux analysis aimed at developing a more comprehensive understanding of the cellular response to ammonium limitation.

CONCLUSIONS

We have developed and applied a high-performance metabolomic profiling workflow for quantitative yeast metabolomics with high coverage. Dansyl and DmPA labeling have been used to quantify the changes of the amine/phenol submetabolome and the acid submetabolome in yeast cells, respectively. The same workflow should be applicable to profile the submetabolomes of other chemical groups such as ketones, aldehydes, and hydroxyl using new reagents that are currently under development in our laboratory. We demonstrated the utility of this workflow for comparative yeast metabolomics in cells cultured with and without nitrogen limitation. It was found that the abundances of a large number of metabolites were significantly altered in cells cultured with nitrogen limitation, proving the importance of performing metabolomic profiling with high sensitivity and accuracy. Among the metabolic pathway changes examined, our results suggest that systems engineering of acetyl-CoA production in yeast might benefit from manipulation of the links between ammonium assimilation and accumulation of pantothenate, which is an essential precursor of acetyl-CoA.

ASSOCIATED CONTENT

Supporting Information

The Supporting Information is available free of charge on the ACS Publications website at DOI: 10.1021/acs.jproteome.6b00070.

Table S1: amine- or phenol-containing metabolites positively identified using accurate mass and retention time match to a dansyl standards library. Table S2: amine- or phenol-containing metabolites putatively identified based on accurate mass search against the HMDB library. Table S3: amine- or phenol-containing metabolites putatively identified based on accurate mass search against the MCID library with one reaction. Table S4−1: amine- or phenol-containing metabolites putatively identified based on accurate mass search against the YMDB library. Table S4−2: acid-containing metabolites putatively identified based on accurate mass search against the YMDB library. Table S5−1: metabolites positively identified that show significant changes. Table S5−2: amine- or phenol-containing metabolites putatively identified that show significant changes. Table S5−3: acid-containing metabolites putatively identified that show significant changes. Table S6: acid-containing metabolites positively identified based on accurate mass and retention time search against a DmPA standards library. Table S7: acid-containing metabolites putatively identified based on accurate mass search against the HMDB library. Table S8: acid-containing metabolites putatively identified based on accurate mass search against the MCID library with one reaction. (ZIP)

AUTHOR INFORMATION

Corresponding Author

*Tel: 780-492-3250; fax: 780-492-8231; e-mail: Liang.Li@ualberta.ca.

Notes

The authors declare no competing financial interest.

ACKNOWLEDGMENTS

This work was supported by grants from the Natural Sciences and Engineering Research Council of Canada (LL), Canadian Institutes of Health Research (MCS), the Canada Research Chairs program (LL), Genome Canada (LL), and Alberta Innovates (LL). We thank Gareth Lambkin (Biological Services, University of Alberta) for his assistance in cell culture.

REFERENCES

(1) Botstein, D.; Fink, G. R. Yeast: An Experimental Organism for 21st Century Biology. *Genetics* **2011**, *189* (3), 695−704.

(2) Legras, J. L.; Merdinoglu, D.; Cornuet, J. M.; Karst, F. Bread, beer and wine: Saccharomyces cerevisiae diversity reflects human history. *Mol. Ecol.* **2007**, *16* (10), 2091−2102.

(3) Dequin, S. The potential of genetic engineering for improving brewing, wine-making and baking yeasts. *Appl. Microbiol. Biotechnol.* **2001**, *56* (5−6), 577−588.

(4) Oud, B.; Maris, A. J. A.; Daran, J. M.; Pronk, J. T. Genome-wide analytical approaches for reverse metabolic engineering of industrially relevant phenotypes in yeast. *FEMS Yeast Res.* **2012**, *12* (2), 183−196.

(5) Mattanovich, D.; Sauer, M.; Gasser, B. Yeast biotechnology: teaching the old dog new tricks. *Microb. Cell Fact.* **2014**, *13*, 34.

(6) Nielsen, J. Yeast cell factories on the horizon. *Science* **2015**, *349* (6252), 1050−1051.

(7) Ellis, D. I.; Goodacre, R. Metabolomics-assisted synthetic biology. *Curr. Opin. Biotechnol.* **2012**, *23* (1), 22−28.

(8) Dromms, R. A.; Styczynski, M. P. Systematic Applications of Metabolomics in Metabolic Engineering. *Metabolites* **2012**, *2* (4), 1090−1122.

(9) Joyner, P. M.; Matheke, R. M.; Smith, L. M.; Cichewicz, R. H. Probing the Metabolic Aberrations Underlying Mutant Huntingtin Toxicity in Yeast and Assessing Their Degree of Preservation in Humans and Mice. *J. Proteome Res.* **2010**, *9* (1), 404−412.

(10) Yu, S. L.; An, Y. J.; Yang, H. J.; Kang, M. S.; Kim, H. Y.; Wen, H.; Jin, X.; Kwon, H. N.; Min, K. J.; Lee, S. K.; Park, S. Alanine-Metabolizing Enzyme Alt1 Is Critical in Determining Yeast Life Span, As Revealed by Combined Metabolomic and Genetic Studies. *J. Proteome Res.* **2013**, *12* (4), 1619−1627.

(11) Airoldi, C.; Tripodi, F.; Guzzi, C.; Nicastro, R.; Coccetti, P. NMR analysis of budding yeast metabolomics: a rapid method for sample preparation. *Mol. BioSyst.* **2015**, *11* (2), 379−383.

(12) Kondo, E.; Marriott, P. J.; Parker, R. M.; Kouremenos, K. A.; Morrison, P.; Adams, M. Metabolic profiling of yeast culture using gas chromatography coupled with orthogonal acceleration accurate mass time-of-flight mass spectrometry: Application to biomarker discovery. *Anal. Chim. Acta* **2014**, *807*, 135−142.

(13) Carneiro, S.; Pereira, R.; Rocha, I. Yeast Metabolomics: Sample Preparation for a GC/MS-Based Analysis. In *Yeast Metabolic Engineering: Methods and Protocols*, Mapelli, V., Ed. Humana Press Inc: Totowa, 2014; Vol. *1152*, pp 197−207.

(14) Klavins, K.; Drexler, H.; Hann, S.; Koellensperger, G. Quantitative Metabolite Profiling Utilizing Parallel Column Analysis for Simultaneous Reversed-Phase and Hydrophilic Interaction Liquid Chromatography Separations Combined with Tandem Mass Spectrometry. *Anal. Chem.* **2014**, *86* (9), 4145−4150.

(15) Farres, M.; Pina, B.; Tauler, R. Chemometric evaluation of Saccharomyces cerevisiae metabolic profiles using LC-MS. *Metabolomics* **2015**, *11* (1), 210−224.

DOI: 10.1021/acs.jproteome.6b00070
J. Proteome Res. 2016, 15, 1602−1612

(16) Li, K. F.; Wang, X.; Pidatala, V. R.; Chang, C. P.; Cao, X. H. Novel Quantitative Metabolomic Approach for the Study of Stress Responses of Plant Root Metabolism. *J. Proteome Res.* **2014**, *13* (12), 5879−5887.
(17) Ito, Y.; Hirasawa, T.; Shimizu, H. Metabolic engineering of Saccharomyces cerevisiae to improve succinic acid production based on metabolic profiling. *Biosci., Biotechnol., Biochem.* **2014**, *78* (1), 151−159.
(18) Venter, L.; Lindeque, Z.; Jansen van Rensburg, P. J.; van der Westhuizen, F.; Smuts, I.; Louw, R. Untargeted urine metabolomics reveals a biosignature for muscle respiratory chain deficiencies. *Metabolomics* **2015**, *11* (1), 111−121.
(19) Guo, K.; Li, L. Differential C-12/C-13-Isotope Dansylation Labeling and Fast Liquid Chromatography/Mass Spectrometry for Absolute and Relative Quantification of the Metabolome. *Anal. Chem.* **2009**, *81* (10), 3919−3932.
(20) Guo, K.; Li, L. High-Performance Isotope Labeling for Profiling Carboxylic Acid-Containing Metabolites in Biofluids by Mass Spectrometry. *Anal. Chem.* **2010**, *82* (21), 8789−8793.
(21) Magasanik, B.; Kaiser, C. A. Nitrogen regulation in Saccharomyces cerevisiae. *Gene* **2002**, *290* (1−2), 1−18.
(22) Ljungdahl, P. O.; Daignan-Fornier, B. Regulation of Amino Acid, Nucleotide, and Phosphate Metabolism in Saccharomyces cerevisiae. *Genetics* **2012**, *190* (3), 885−929.
(23) Saldanha, A. J.; Brauer, M. J.; Botstein, D. Nutritional Homeostasis in Batch and Steady-State Culture of Yeast. *Mol. Biol. Cell* **2004**, *15* (9), 4089−4104.
(24) Runguphan, W.; Keasling, J. D. Metabolic engineering of Saccharomyces cerevisiae for production of fatty acid-derived biofuels and chemicals. *Metab. Eng.* **2014**, *21*, 103−113.
(25) Kamisaka, Y.; Noda, N.; Tomita, N.; Kimura, K.; Kodaki, T.; Hosaka, K. Identification of genes affecting lipid content using transposon mutagenesis in Saccharomyces cerevisiae. *Biosci., Biotechnol., Biochem.* **2006**, *70* (3), 646−653.
(26) Treco, D. A.; Lundblad, V. Basic techniques of yeast genetics. In *Current Protocols in Molecular Biology*; Ausubel, F. M, Brent, B., Kingston, R. E., Moore, D. D., Seidman, J. G., Ed. John Wiley and Sons: New York, 1993; pp 13.11.11−13.11.17.
(27) Baker Brachmann, C. B.; Davies, A.; Cost, G. J.; Caputo, E.; Li, J. C.; Hieter, P.; Boeke, J. D. Designer deletion strains derived from Saccharomyces cerevisiae S288C: a useful set of strains and plasmids for PCR-mediated gene disruption and other applications. *Yeast* **1998**, *14* (2), 115−132.
(28) Steinle, A.; Bergander, K.; Steinbuchel, A. Metabolic Engineering of Saccharomyces cerevisiae for Production of Novel Cyanophycins with an Extended Range of Constituent Amino Acids. *Appl. Environ. Microbiol.* **2009**, *75* (11), 3437−3446.
(29) Chen, B.; Lee, D.-Y.; Chang, M. W. Combinatorial metabolic engineering of Saccharomyces cerevisiae for terminal alkene production. *Metab. Eng.* **2015**, *31*, 53−61.
(30) Reyes, L. H.; Gomez, J. M.; Kao, K. C. Improving carotenoids production in yeast via adaptive laboratory evolution. *Metab. Eng.* **2014**, *21*, 26−33.
(31) Wang, P. P.; Wei, Y. J.; Fan, Y.; Liu, Q. F.; Wei, W.; Yang, C. S.; Zhang, L.; Zhao, G. P.; Yue, J. M.; Yan, X.; Zhou, Z. H. Production of bioactive ginsenosides Rh2 and Rg3 by metabolically engineered yeasts. *Metab. Eng.* **2015**, *29*, 97−105.
(32) Steen, E.; Chan, R.; Prasad, N.; Myers, S.; Petzold, C.; Redding, A.; Ouellet, M.; Keasling, J. Metabolic engineering of Saccharomyces cerevisiae for the production of n-butanol. *Microb. Cell Fact.* **2008**, *7* (1), 36.
(33) Hanscho, M.; Ruckerbauer, D. E.; Chauhan, N.; Hofbauer, H. F.; Krahulec, S.; Nidetzky, B.; Kohlwein, S. D.; Zanghellini, J.; Natter, K. Nutritional requirements of the BY series of Saccharomyces cerevisiae strains for optimum growth. *FEMS Yeast Res.* **2012**, *12* (7), 796−808.
(34) Cohen, R.; Engelberg, D. Commonly used Saccharomyces cerevisiae strains (e.g. BY4741, W303) are growth sensitive on synthetic complete medium due to poor leucine uptake. *FEMS Microbiol. Lett.* **2007**, *273* (2), 239−243.
(35) Yanes, O.; Tautenhahn, R.; Patti, G. J.; Siuzdak, G. Expanding Coverage of the Metabolome for Global Metabolite Profiling. *Anal. Chem.* **2011**, *83* (6), 2152−2161.
(36) Peng, J.; Li, L. Liquid-liquid extraction combined with differential isotope dimethylaminophenacyl labeling for improved metabolomic profiling of organic acids. *Anal. Chim. Acta* **2013**, *803*, 97−105.
(37) Wu, Y. M.; Li, L. Determination of Total Concentration of Chemically Labeled Metabolites as a Means of Metabolome Sample Normalization and Sample Loading Optimization in Mass Spectrometry-Based Metabolomics. *Anal. Chem.* **2012**, *84* (24), 10723−10731.
(38) Zhou, R.; Tseng, C. L.; Huan, T.; Li, L. IsoMS: Automated Processing of LC-MS Data Generated by a Chemical Isotope Labeling Metabolomics Platform. *Anal. Chem.* **2014**, *86* (10), 4675−4679.
(39) Huan, T.; Li, L. Counting Missing Values in a Metabolite-Intensity Data Set for Measuring the Analytical Performance of a Metabolomics Platform. *Anal. Chem.* **2015**, *87* (2), 1306−1313.
(40) Huan, T.; Wu, Y.; Tang, C.; Lin, G.; Li, L. DnsID in MyCompoundID for Rapid Identification of Dansylated Amine- and Phenol-Containing Metabolites in LC−MS-Based Metabolomics. *Anal. Chem.* **2015**, *87* (19), 9838−9845.
(41) Li, L.; Li, R. H.; Zhou, J. J.; Zuniga, A.; Stanislaus, A. E.; Wu, Y. M.; Huan, T.; Zheng, J. M.; Shi, Y.; Wishart, D. S.; Lin, G. H. MyCompoundID: Using an Evidence-Based Metabolome Library for Metabolite Identification. *Anal. Chem.* **2013**, *85* (6), 3401−3408.
(42) Han, J.; Gagnon, S.; Eckle, T.; Borchers, C. H. Metabolomic analysis of key central carbon metabolism carboxylic acids as their 3-nitrophenylhydrazones by UPLC/ESI-MS. *Electrophoresis* **2013**, *34* (19), 2891−2900.
(43) Cardaci, S.; Ciriolo, M. R. TCA Cycle Defects and Cancer: When Metabolism Tunes Redox State. *Int. J. Cell Biol.* **2012**, *2012*, 1−9.
(44) Brauer, M. J.; Yuan, J.; Bennett, B. D.; Lu, W.; Kimball, E.; Botstein, D.; Rabinowitz, J. D. Conservation of the metabolomic response to starvation across two divergent microbes. *Proc. Natl. Acad. Sci. U. S. A.* **2006**, *103* (51), 19302−7.
(45) Liu, B. S.; Sutton, A.; Sternglanz, R. A yeast polyamine acetyltransferase. *J. Biol. Chem.* **2005**, *280* (17), 16659−16664.
(46) Mandal, S.; Mandal, A.; Johansson, H. E.; Orjalo, A. V.; Park, M. H. Depletion of cellular polyamines, spermidine and spermine, causes a total arrest in translation and growth in mammalian cells. *Proc. Natl. Acad. Sci. U. S. A.* **2013**, *110* (6), 2169−2174.
(47) Olzhausen, J.; Schubbe, S.; Schuller, H. J. Genetic analysis of coenzyme A biosynthesis in the yeast Saccharomyces cerevisiae: identification of a conditional mutation in the pantothenate kinase gene CAB1. *Curr. Genet.* **2009**, *55* (2), 163−73.
(48) Chen, Y.; Siewers, V.; Nielsen, J. Profiling of Cytosolic and Peroxisomal Acetyl-CoA Metabolism in Saccharomyces cerevisiae. *PLoS One* **2012**, *7* (8), e42475.
(49) Nielsen, J. Synthetic Biology for Engineering Acetyl Coenzyme A Metabolism in Yeast. *mBio* **2014**, *5* (6), e02153-14.
(50) Zhou, Y. J.; Buijs, N. A.; Siewers, V.; Nielsen, J. Fatty Acid-Derived Biofuels and Chemicals Production in Saccharomyces cerevisiae. *Front. Bioeng. Biotechnol.* **2014**, *2*, 32.
(51) Kozak, B. U.; van Rossum, H. M.; Luttik, M. A. H.; Akeroyd, M.; Benjamin, K. R.; Wu, L.; de Vries, S.; Daran, J. M.; Pronk, J. T.; van Maris, A. J. A. Engineering Acetyl Coenzyme A Supply: Functional Expression of a Bacterial Pyruvate Dehydrogenase Complex in the Cytosol of Saccharomyces cerevisiae. *mBio* **2014**, *5* (5), e01696-14.
(52) Lian, J. Z.; Si, T.; Nair, N. U.; Zhao, H. M. Design and construction of acetyl-CoA overproducing Saccharomyces cerevisiae strains. *Metab. Eng.* **2014**, *24*, 139−149.
(53) Terrance, G. C. Nitrogen Metabolism in Saccharomyces cerevisiae. In *The Molecular Biology of the Yeast Saccharomyces: Metabolism and Gene Expression*, Volume *11B*; Cold Spring Harbor Laboratory Press: Woodbury, NY, **1982**.

DOI: 10.1021/acs.jproteome.6b00070
J. Proteome Res. 2016, 15, 1602−1612